Selecting Time-Frequency Representations for Detecting Rotor Faults in BLDC Motors Operating Under Rapidly Varying Operating Conditions

Satish Rajagopalan[1] José A. Restrepo[2] José M. Aller[2] Thomas G. Habetler[1] Ronald G. Harley[1]

[1]Georgia Institute of Technology
Atlanta, Georgia 30332, USA.
thabetler@ece.gatech.edu

[2]Universidad Simón Bolívar
Caracas 1080A, VENEZUELA.
restrepo@usb.ve

***Abstract* – Electric motors work continuously under operating conditions that rapidly vary with time. Motor diagnostics in a non-stationary environment is challenging due to the need for sophisticated signal processing techniques. In this paper, the use of quadratic TFRs is presented as a solution for the diagnostics of rotor faults in Brushless DC (BLDC) motors operating under constantly changing load and speed conditions. Four time-frequency representations are considered in this paper – short-time Fourier transform (STFT), Wigner-Ville distribution (WVD), Choi-Williams Distribution (CWD), and the Zhao-Atlas Marks Distribution (ZAM). The drawbacks of these distributions and methods to overcome them are also presented. The TFRs are implemented in real-time and their load computations are compared in order to study their suitability for implementation in a commercial system.**

I. INTRODUCTION

Operating conditions of an electric motor usually change rapidly over time. Diagnostics of motor faults in such conditions is a challenging problem due to the need for application of sophisticated signal processing techniques that can process non-stationary signals. Extensive research has been reported in the area of fault detection in electric motors operating under fixed speed and load conditions [1-3]. While some research has been reported in the detection of faults in induction motors operating under very slowly varying speed and load conditions [4,5], no research has been reported in the diagnosis of faults in motors operating under rapidly varying operating conditions.

The classical technique for characterizing the time evolution of non-stationary signals is the short-time Fourier transform (STFT), a linear time frequency representation (TFR). Though simple and rugged, the STFT still assumes that the non-stationary signal is slowly changing in the chosen time window. This and the choice of window length impair the use of STFT at low frequencies or when the signal is highly dynamic. Beginning with the Wigner-Ville distribution a plethora of quadratic TFR techniques have been introduced in an attempt to improve the time-frequency detail over that achievable with the STFT [6]. They have been extensively used in the area of mechanical engineering for detection of gear faults. The use of TFRs in the detection of faults in industrial frequency converters has also been reported [7]. Another application where TFRs have been used is in the analysis of induction machine slot harmonics in the transient state [8].

In this paper, the use of quadratic TFRs is proposed as a solution for the diagnostics of rotor faults in electric motors operating under non-stationary load and speed conditions. Although the method could be applied to any motor, its application is limited in this paper to BLDC motors. Four time-frequency representations are considered in this paper – short-time Fourier transform (STFT), Wigner-Ville distribution (WVD), Choi-Williams Distribution (CWD), and the Zhao-Atlas Marks Distribution (ZAM). The pros and cons of these distributions are analyzed and techniques to overcome them are presented. The TFRs are implemented in on a digital signal processor (DSP) and their load computations are compared in order to determine their suitability for implementation in a real system.

II. GENERALIZED T-F DISTRIBUTIONS

Time-frequency analysis is the three-dimensional time, frequency, and amplitude representation of a signal, which is inherently suited to indicate transient events in a signal. They thus combine time-domain and frequency-domain analysis to yield a more revealing picture of the temporal localization of a signal's spectral component. A special class of distributions, commonly referred to as Generalized Time Frequency distributions (GTFRDs) or members of the Cohen class have been widely researched in recent times [9]. These distributions can be used for the analysis for true non-stationary signals without any underlying assumptions. The Cohen class of distributions for a signal *s(t)* are given by

$$\rho(t,f) = \iiint e^{j2\pi v(u-t)} g(v,\tau) \times s^*\left(u-\frac{\tau}{2}\right) s\left(u+\frac{\tau}{2}\right) e^{-j2\pi f\tau}\, dv\, du\, d\tau \quad (1)$$

where $g(v,\tau)$ is an arbitrary function called the kernel. Setting the kernel $g(v,\tau) = 1$ yields the well known Wigner-Ville distribution (WVD). However, the biggest drawback of quadratic distributions such as the WVD is the introduction of non-negligible cross-term artifacts. The cross-term can be suppressed by using more complicated kernels such as the CWD or the ZAM, however at the cost of frequency resolution. Table 1 depicts some commonly used TFRs and their respective kernels, where $h(\tau)$ is a time window (Gaussian, Hamming,…) and σ in the CWD is a parameter that determines the trade-off between cross-term suppression and frequency resolution [10]. The CWD is an exponential kernel that effectively suppresses cross-terms [11]. The ZAM on the other hand is a newer distribution that significantly enhances the time and frequency resolution while suppressing the cross-terms [12]. The PWVD is the windowed version of the WVD. The PWVD may be defined in the time domain or in the frequency domain, though the former is more common. Also called the Windowed-Wigner

distribution, the PWVD suppresses cross-terms present in the original Wigner distribution but has poor frequency resolution. Another distribution not shown in Table 1 is the Smoothed PWVD (SPWVD). The smoothed WVD (SPWVD) uses a smoothing function that smoothes the distribution in both the time and frequency planes. The SPWVD offers better cross-term suppression than the PWVD but again suffers from reduced frequency resolution.

TABLE I
SELECTED TFRS AND THEIR KERNELS

TFR	**Kernel: *g(ν, τ)***
WVD	1
PWVD (Windowed WVD)	$h(\tau)$
CWD	$e^{-v^2\tau^2}/\sigma$
ZAM	$\frac{\sin\left(2\pi v\lvert\tau\rvert/a\right)}{\pi v};\ a=1$
Spectrogram	$\int h^*\left(u-\frac{\tau}{2}\right)e^{j2\pi vu}\, h\left(u+\frac{\tau}{2}\right)du$

III. TFR-BASED ROTOR FAULT DETECTION IN BLDC MOTORS

Several researchers have shown that rotor defects in induction motors operating at a constant speed affect certain characteristic frequency components in the machine stator current and such rotor defects can be identified by monitoring the amplitude of these harmonic components [2]. This popular method is called Motor Current Signature Analysis (MCSA) [3]. In BLDC motors operating at constant speed, these frequencies are given by, [13]

$$f_{rf} = f_e \pm k\frac{f_e}{P/2}. \tag{2}$$

where, f_{rf} is the rotor fault frequency, f_e is the fundamental frequency, P is the number of poles in the BLDC machine, and k is any integer. These fault frequencies are also present when the current is in a non-stationary state and will be tracked using the proposed TFR based detection algorithm.

The acquired BLDC stator current is first filtered adaptively to remove the fundamental frequency and other inverter harmonics. This selective adaptive filtering prevents cross-terms from being introduced at frequencies of interest. The filtered stator current is then converted into an analytic signal using a Hilbert transformation [10]. The analytic signal of a real-valued signal *s(t)* is defined as

$$s_A(t) = s(t) + js_H(t). \tag{3}$$

where $s_H(t)$ is the Hilbert transform of *s(t)* and is given by

$$H\left[s(t)\right] = s_H(t) = \frac{1}{\pi}\int_{-\infty}^{\infty} s(\tau)\frac{1}{t-\tau}d\tau \tag{4}$$

The TFR is then calculated for a time slice of predetermined length. The length is usually a power of 2 to facilitate fast computation. The fault frequencies obtained from the TFR is then used to compute a fault metric that indicates the health of the motor.

IV. COMPARISON OF VARIOUS TFRS

A hypothetical test signal, i_a, approximating a rotor fault scenario and having a fundamental of amplitude 0.04 A (corresponding to a filtered stator current) with two rotor fault sidebands of amplitude 0.05 A is generated using (5). The three frequencies in (5) are the fundamental frequency *p(t)* and two rotor fault frequencies at 2/3rd and 4/3rd of the fundamental frequency *p(t)*.

$$\begin{aligned} i_a &= 0.04\cos\left(2\pi p(t)t\right) + 0.05\cos\left(4\pi p(t)t/3\right) \\ &\quad + 0.05\cos\left(8\pi p(t)t/3\right) \end{aligned} \tag{5}$$

The frequency *p(t)* is varied sinusoidally between 0 and 120 Hz. The Rice University Time Frequency Analysis toolbox [14] for MATLAB is used to compute the Wigner distributions for the simulated motor current signal. Figure 1 shows the spectrogram (STFT) of the signal. Darker zones in the scalogram represent higher amplitudes. The window *h(τ)* of the spectrogram in Table 1 is chosen as a Hamming window of length 0.25 seconds. The frequency resolution of the spectrogram is poor in the low frequency region as the three frequencies of (5) can not be distinguished from each other as the fundamental frequency drops below 60 Hz. It can also be seen from Figure 1 that the spectral components produced by the STFT are smeared (or thick) in the frequency domain. Hence the fault frequencies are not localized but spread over a frequency range. Figure 2 shows the PWVD of the test signal i_a. The frequencies are concentrated in a thin band indicating excellent concentration of energy but the presence of strong cross-terms may produce false fault alarms. The CWD in Figure 3 (σ =1) has better energy concentration than the STFT, but the frequency resolution in the low frequency region (below 50 Hz) is compromised to obtain good cross-term suppression.

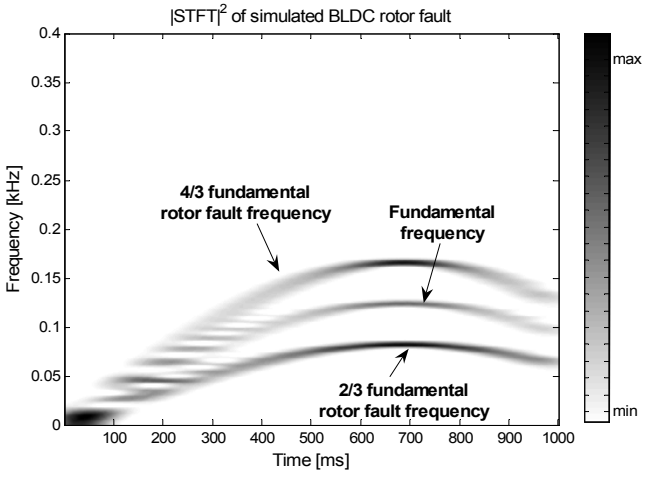

Fig. 1. STFT of simulated BLDCM rotor fault.

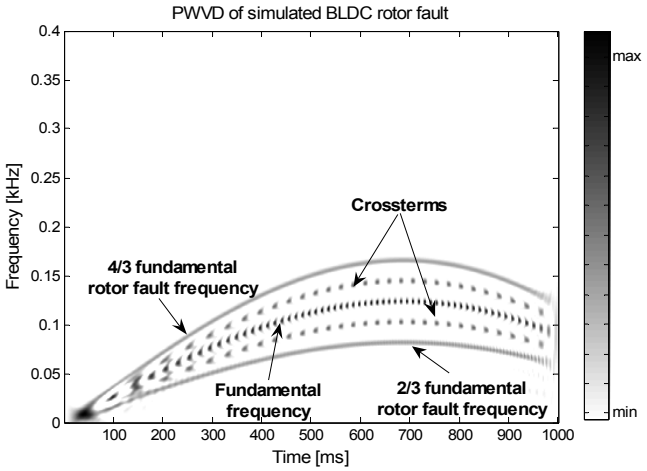

Fig. 2. PWVD of simulated BLDCM rotor fault.

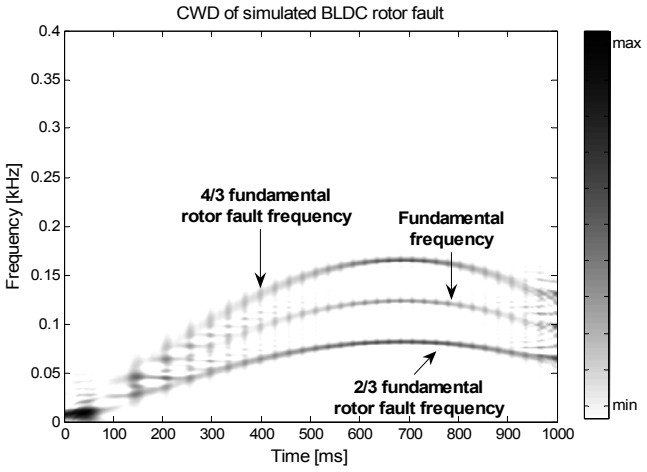

Fig. 3. CWD of simulated BLDCM rotor fault.

The ZAM distribution in Figure 4 shows good energy concentration (low frequency smear), excellent cross-term suppression and much better frequency resolution than the STFT. The PWVD, CWD, and the ZAM distribution are calculated from the Hilbert transformed analytic version of the simulated real-valued current signal generated by (5). The use of the analytic signal instead of the real valued signal itself helps in mitigating cross-terms and ghosts to a large extent. The Hilbert transform is implemented in MATLAB using standard MATLAB functions.

V. EXPERIMENTAL RESULTS

A six-pole 12 V, 1 kW BLDC motor with speed and current control is used in the experiments. One of the phase currents is sensed using a Hall current sensor. The fundamental and harmonics greater than two are adaptively filtered using a 6th order analog switched capacitor tracking filter. Clocking for the filter is obtained from the BLDC motor's Hall position sensors using a Phase Locked Loop (PLL). The filter is fabricated on a 4-layer printed circuit board to obtain noise- free performance. The experimental

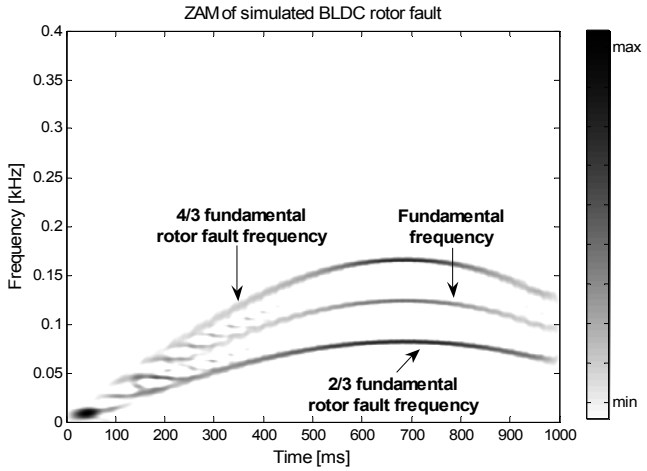

Fig. 4. ZAM of simulated BLDCM rotor fault.

arrangement is shown in Figure 5. For a six-pole BLDC motor, the rotor fault frequencies occur at 1/3rd, 2/3rd, 4/3rd, and 5/3rd times the fundamental frequency (2).

Non-stationary operation is implemented using sinusoidal and triangular speed references of 0 to 15 Hz. This frequency range adequately represents the non-stationarity encountered in several practical applications. The speed is varying from 600 rpm to 1800 rpm. Experimental results are presented for a motor with a dynamic eccentricity of 32% of the air-gap length. In the case of dynamic eccentricity, the centre of the rotor is not at the centre of rotation, and the position of the minimum air-gap rotates with the rotor. This misalignment may be caused by several factors such as misalignment of bearings, mechanical resonance at critical speeds, a bent rotor shaft, or worn bearings.

The stator current of a BLDC motor operating in non-stationary condition is shown in Figure 6. The CWD of the filtered stator current of the dynamically eccentric BLDC motor operating with a 5 Hz sinusoidal speed reference is shown in Figure 7. The fundamental is completely absent as a 60dB Butterworth filter is used to remove the fundamental completely. The two fault frequencies in Figure 7 are seen to be tracked distinctly over time. Figure 8 shows the ZAM distribution of the filtered stator current of a BLDC motor now operating with a 5 Hz triangular speed reference. Again, the ZAM distribution tracks the fault frequencies distinctly over time. Unlike the STFT, no assumption of local stationarity is needed for the CWD and ZAM distributions. These distributions are inherently suited for analyzing non-stationary signals and do not suffer from the problems of window types and size as in the STFT. The amplitude of the extracted fault frequencies can be monitored to detect the occurrence of a rotor fault.

Figure 9 shows a simple fault metric calculated using the RMS of the fault frequency amplitudes extracted using the CWD from the filtered stator current of a good BLDC motor and a faulty BLDC motor with dynamic eccentricity, both operating with a 5 Hz triangular speed reference. The RMS fault metric of the defective BLDC motor can be seen to be much higher than the RMS fault metric of a good motor.

This fault metric can be used as an indicator for automatic detection of rotor faults in BLDC motors.

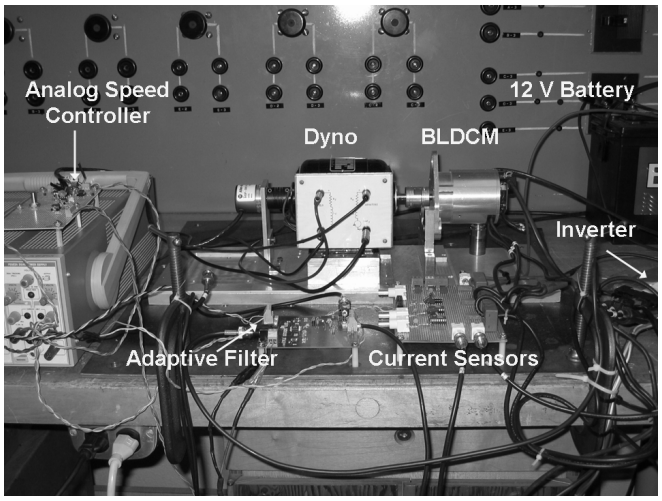

Fig. 5. Experimental arrangement for testing dynamic eccentricity.

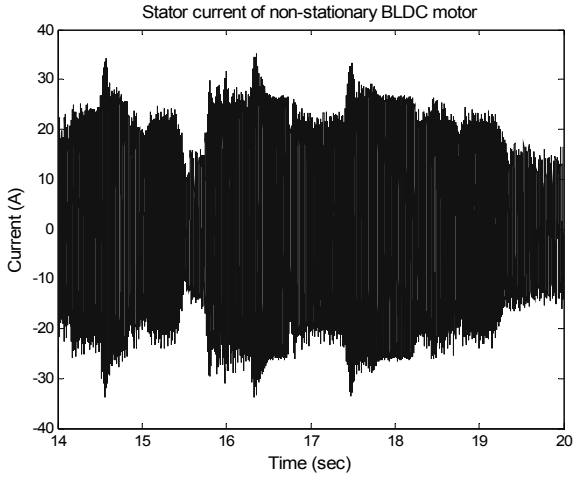

Fig. 6. Non-stationary stator current in a BLDC motor.

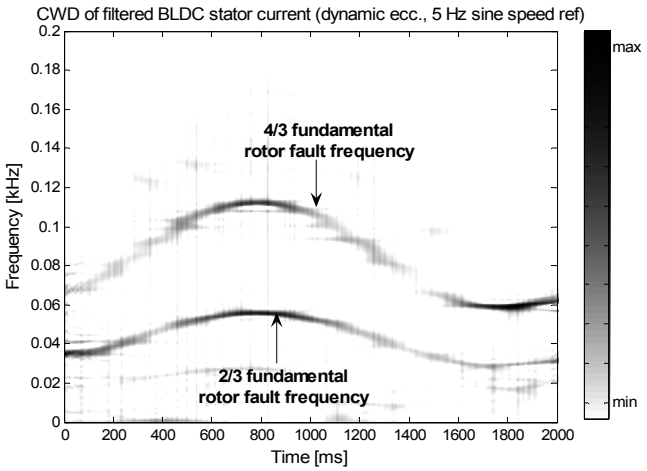

Fig. 7. CWD of filtered BLDC motor (with dynamic eccentricity) stator current and 5 Hz sine speed reference.

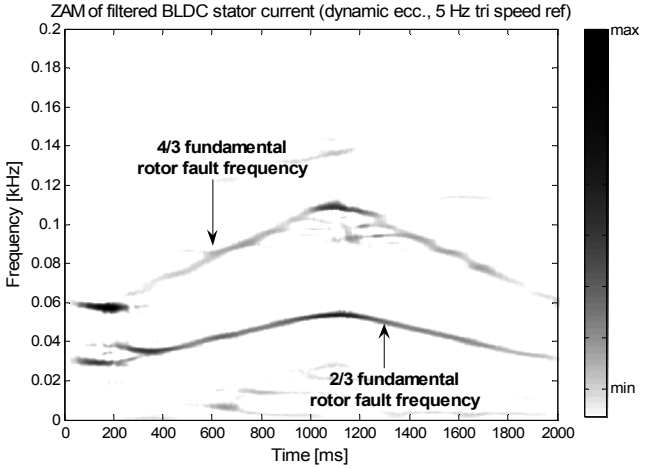

Fig. 8. ZAM of filtered BLDC motor (with dynamic eccentricity) stator current and 5 Hz triangular speed reference..

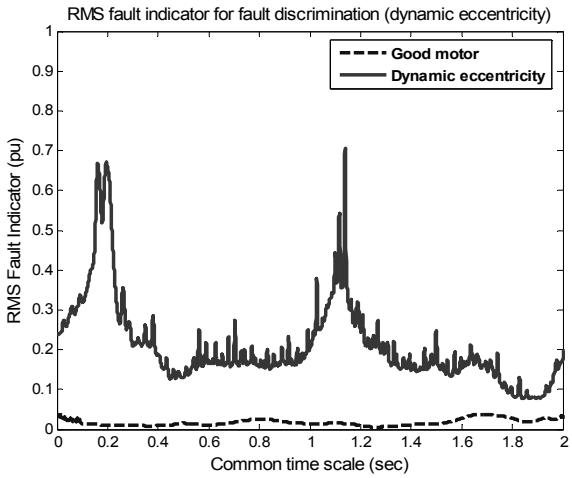

Fig. 9. RMS fault indicator discriminates BLDC rotor eccentricity (5 Hz triangular speed ref).

VI. COMPARISON OF REAL-TIME IMPLEMENTABILITY AND COMPUTATIONAL LOAD

The most important factor in designing any real-time signal processor is the computational load. The spectrogram, WVD, and the CWD are compared for their suitability for implementation in a commercial system. To this effect, the three algorithms are implemented on an ADSP-21061-SHARC DSP operating with a 50 MHz clock and capable of 150 MFLOPS. The ADSP-21061 is a 32-bit floating point processor optimized for high performance DSP applications. The algorithms are first written in C language. The ZAM distribution is not implemented due to the computational complexity involved.

For practical implementation of distributions members of Cohen's class, the generalized discrete-time discrete-frequency distribution (GDTDFD) is defined as [15]:

$$\hat{\mathrm{P}}\left(l,\theta;\hat{\Phi}\right)=\sum_{n=-\infty}^{+\infty}R_l\left(n\right)e^{-j2n\theta} \qquad (6)$$

where the auto-correlation sequence R_l is,

$$R_l(n) = \sum_{m=-\infty}^{+\infty} s(l+m+n)s^*(l+m-n)\hat{\Phi}(m,2n) \quad (7)$$

$\hat{\Phi}$ (m, $2n$) is the discrete-domain kernel that defines the time-frequency representation. In practice only a finite span in time of the signal is available. This can be represented by applying a sliding window to the signal under analysis, so that equations (6) and (7) can be rewritten as follows:

$$\hat{\mathrm{P}}(l,\theta;\hat{\Phi}) = \sum_{n=-N}^{+N} R_l(n)e^{-j2n\theta} \quad (8)$$

and

$$R_l(n) = \sum_{m=-N}^{+N} s(l+m+n)s^*(l+m-n)\hat{\Phi}(m,2n) \quad (9)$$

A. Discrete Wigner-Ville distribution (DWVD)

For the Wigner distribution the discrete-domain kernel is given by

$$\hat{\Phi}(m,2n) = \delta(m). \quad (10)$$

Replacing this in the (9)

$$R_l^{WD} = s(l+n)s^*(l-n). \quad (11)$$

The auto-correlation sequence is first computed and the discrete Fourier transform (DFT) is computed to obtain the DWVD of the sequence. The DWVD can be efficiently computed using standard Fast Fourier transform (FFT) algorithms. The computation is further optimized by evaluating two successive R_l sequences together [16]:

$$R_{comb}^{WD} = R_{l1}(n) + j\,R_{l2}(n) \quad (12)$$

The discrete Fourier transform (DFT) of the individual sequences can be evaluated using a single DFT for the combined kernel, thus halving the number of final FFTs used. The Hilbert transform is implemented as a 79-tap FIR filter [16].

B. Discrete Choi-Williams distribution (DCWD)

Here the exponential CWD kernel (Table 1) is selected in the original domain, and then a Fourier transform is performed along one of its axis to get the kernel in the ambiguity domain. Thus a new correlation vector is constructed and from there the same algorithm used in the WVD is applied.

C. Comparing load computations

The load computations for one time slice of data processed is measured on an oscilloscope and is compared in Table 2. It can be seen that the load computations increase as more complex kernels such as the CWD are used. The spectrogram is implemented using a Gaussian window of length of 0.0625 seconds. The length of the window was chosen heuristically to best fit this application. While the WVD takes almost 4 times the computation time of the spectrogram, more sophisticated distributions like the CWD take about 50 times the computational time of the spectrogram. However, the WVD and CWD yield much better frequency resolution and localization and do not suffer from the problems related to the type and size of the window as in the spectrogram.

TABLE 2
COMPUTATION TIME FOR SELECTED TFR KERNELS

TFR	**Computation time per time slice (μ-sec)**
Spectrogram	0.46
WVD	2.02
CWD	27.93

VII. CONCLUSIONS

The use of time-frequency distributions has proved suitable for detection of rotor faults in electric motors operating under continuous non-stationary conditions. However, the need to provide high frequency resolution along with good cross-term suppression leads to complicated kernels requiring large amounts of processing power. Some of the commonly used TFRs are implemented on a DSP platform to study their computational loads. It is observed that quadratic TFRs such as WVD and CWD are computationally more intensive than linear TFRs such as the spectrogram. The quadratic TFRs however provide much better frequency resolution and localization of energy with the ZAM distribution exhibiting the best performance. The CWD in particular is a good trade-off between the excellent frequency resolution of the WVD and the high cross-term suppression of the ZAM distribution. These distributions also do not depend on the size and type of the window as in the spectrogram.

The increased computational load is the price paid if a better frequency resolution and good localization of energy is needed. In spite of the increased complexity involved, the computation time of a CWD is still in the order of a few tens of micro-seconds and hence is amenable to implementation in real-time. This computational time can be further decreased by paralleling several micro-programmed systems and using more optimized software routines. Newer processors run at much higher speeds and can decrease the computation time by as much as ten times. However, as motor diagnostics is performed over long intervals of time, the computation time may not be very critical and hence most of the quadratic TFRs can be effectively used.

VIII. ACKNOWLEDGMENT

The authors wish to acknowledge the support of Delphi Corp., Troy, MI, and in particular the help of Dr. Tomy

Sebastian (Delphi Saginaw Steering Systems), and Drs. Bruno Lequesne and Thomas W. Nehl (Delphi Research Labs) , as well as financial support from the Duke Power Company in Charlotte, North Carolina.

IX. REFERENCES

[l] S. Nandi and H. A. Toliyat, "Condition monitoring and fault diagnosis of electrical machines – A review," in *Proceedings of the 34th Annual Meeting of the IEEE Industry Applications*, 1999, pp. 197-204.

[2] J. M. Cameron, W. T. Thomson, and A. B. Dow, Vibration and current monitoring for detecting airgap eccentricity in large induction motors," *IEE Proceedings*, vol. 133, pt. B, no. 3, 1986, pp.155-163.

[3] G. B. Kliman and J. Stein, "Methods of motor current signature analysis," *Electric Machines and Power Systems*, vol. 20, no. 5, 1992, pp. 463-474.

[4] B. Yazici and G. B. Kliman, "An adaptive statistical time-frequency method for detection of broken bars and bearing faults in motors using stator current," *IEEE Trans. Industry Applications*, vol.35, no. 2, 1999, pp. 442-452.

[5] K. Kim and A. G. Parlos, "Induction motor fault diagnosis based on neuropredictors and wavelet signal processing," *IEEE/ASME Trans. Mechatronics*, vol. 7, no. 2, 2002, pp. 201-219.

[6] S. L. Marple Jr., "Time-frequency signal analysis: issues and alternative methods," in *Proceedings of the IEEE-SP International Symposium on Time-Frequency and Time-Scale Analysis*, 1998, pp. 329-332.

[7] Z. Leonowicz and T. Lobos, "Application of time-frequency distribution and neural networks for fault classification in power electronics," in *Proceedings of the IEEE-SP International Symposium on Computational Intelligence for Measurement Systems and Applications*, 2003, pp. 67-71.

[8] J. A. Restrepo and P. Bowler, "Analysis of induction machine slot harmonics in the TF domain," in *Proceedings of the First IEEE International Caracas Conference on Devices, Circuits and Systems*, 1995, pp. 127-130.

[9] L. Cohen, "Time-frequency distributions – A review," in *Proceedings of the IEEE*, vol. 77, no. 7, 1989, pp. 941-981.

[10] B. Boashash, *Time-Frequency Signal Analysis – Methods and Applications*, Melbourne, Australia: Longman Cheshire, 1992, pp. 26.

[11] H. I. Choi and W. J. Williams, "Improved time-frequency representation of multi-component signals using exponential kernels," *IEEE Trans. on Acoustics, Speech, and Signal Processing*, vol. 37, no. 6, 1989, pp. 862-871.

[12] Y. Zhao, L. E. Atlas, and R. J. Marks II, "The use of cone-shaped kernels for generalized time-frequency representations of nonstationary signals," *IEEE Trans. on Acoustics, Speech, and Signal Processing*, vol. 38, no. 7, 1990, pp. 1084-1091.

[13] S. Rajagopalan, W. le Roux, R.G. Harley and T.G. Habetler, "Diagnosis of potential rotor faults in brushless DC machines," in *Proceedings of the Second International Conference on Power Electronics, Machines and Drives (PEMD 2004)*, 2004, pp. 668-673.

[14] F. Auger, P. Flandrin, P. Goncalvès, and O. Lemoine, *Time-frequency toolbox for use with MATLAB*, CNRS France and Rice University, USA, 1996.

[15] F. Hlawatsch and G. F. Boudreaux-Bartels, "Linear and quadratic time-frequency representations," *IEEE Signal Processing Magazine*, 1992, pp. 21-67.

[16] B. Boashash and P. J. Black, "An efficient real-time implementation of the Wigner-Ville distribution," *IEEE Trans. on Acoustics, Speech, and Signal Processing*, vol. 35, no. 11, 1978, pp. 1611-1618.